Counts of high-redshift GRBs as probe of primordial non-Gaussianities

Umberto Maio[1]⋆, Ruben Salvaterra[2], Lauro Moscardini[3,4,5], and Benedetta Ciardi[6]

[1] *Max-Planck-Institut für extraterrestrische Physik, Giessenbachstraße 1, D-85748 Garching b. München, Germany*

[2] *INAF/IASF - Italian National Astrophysical Institute, via E. Bassini 15, I-20133 Milano, Italy*

[3] *Dipartimento di Astronomia, Università di Bologna, via Ranzani 1, I-40127 Bologna, Italy*

[4] *INAF, Osservatorio Astronomico di Bologna, via Ranzani 1, I-40127 Bologna, Italy*

[5] *INFN, Sezione di Bologna, viale Berti Pichat 6/2, I-40127 Bologna, Italy*

[6] *Max-Planck-Institut für Astrophysik, Karl-Schwarzschild-Straße 1, D-85748 Garching b. München, Germany*

ABSTRACT

We propose to use high-redshift long γ-ray bursts (GRBs) as cosmological tools to constrain the amount of primordial non-Gaussianity in the density field. By using numerical, N-body, hydrodynamic, chemistry simulations of different cosmological volumes with various Gaussian and non-Gaussian models, we self-consistently relate the cosmic star formation rate density to the corresponding GRB rate. Assuming that GRBs are fair tracers of cosmic star formation, we find that positive local non-Gaussianities, described in terms of the non-linear parameter, f_{NL}, might boost significantly the GRB rate at high redshift, $z \gg 6$. Deviations with respect to the Gaussian case account for a few orders of magnitude if $f_{NL} \sim 1000$, one order of magnitude for $f_{NL} \sim 100$, and a factor of ~ 2 for $f_{NL} \sim 50$. These differences are found only at large redshift, while at later times the rates tend to converge. Furthermore, a comparison between our predictions and the observed GRB data at $z > 6$ allows to exclude large negative f_{NL}, consistently with previous works. Future detections of any long GRB at extremely high redshift ($z \sim 15 - 20$) could favor non-Gaussian scenarios with positive f_{NL}. More stringent constraints require much larger high-z GRB complete samples, currently not available in literature. By distinguishing the contributions to the GRB rate from the metal-poor population III regime, and the metal-enriched population II-I regime, we conclude that the latter is a more solid tracer of the underlying matter distribution, while the former is strongly dominated by feedback mechanisms from the first, massive, short-lived stars, rather than by possible non-Gaussian fluctuations. This holds quite independently of the assumed population III initial mass function.

Key words: cosmology: theory – structure formation; gamma-rays: bursts

1 INTRODUCTION

The present standard cosmological model assumes that a primordial inflationary phase (Starobinsky 1980; Guth 1981; Linde 1990) ends with the creation of density fluctuations, that then grow during cosmological times (e.g. Gunn & Gott 1972; Weinberg 1972; Press & Schechter 1974; White & Rees 1978; Peebles, P. J. E. 1993; Sheth & Tormen 1999; Peacock, J. A. 1999; Hogg 1999; Coles, P. & Lucchin, F. 2002; Peebles & Ratra 2003) to give birth to the presently observed large scale structure of the Universe (Barkana & Loeb 2001; Ciardi & Ferrara 2005; Bromm & Yoshida 2011). Stars, galaxies, and clusters of galaxies form by gravitational collapse in an expanding flat space, composed by $\sim 30\%$ of matter and $\sim 70\%$ of an unknown constituent referred to as dark energy,

for which the cosmological constant Λ represents the simplest explanation. Thanks to the evidences coming from different observational datasets (mainly cosmic microwave background, galaxy surveys and supernovae), the general properties of our Universe have become clearer and its parameters known with much better accuracy. The estimated contributions to the cosmic density are (Komatsu et al. 2011): $\Omega_{0,m} = 0.272$, $\Omega_{0,\Lambda} = 0.728$, $\Omega_{0,b} = 0.044$, for matter, cosmological constant, and baryons, respectively; the cosmic equation of state parameter is consistent with $w = -1$, the theoretical expectation of the cosmological constant; the primordial power spectrum has spectral index $n = 0.96$, and a normalization corresponding to a mass variance within a $8 \, \mathrm{Mpc}/h$-sphere of $\sigma_8 = 0.8$.

Even if the above picture is quite satisfying, the specific mechanism driving the inflation is however not completely understood. This fact justifies the existence in the literature of a plethora of

⋆ E-mail: umaio@mpe.mpg.de

possible inflationary models, each of them with specific predictions for various observables. In particular, the study of the statistical distribution of the primordial fluctuations is considered one of the best way to discriminate between them. In fact, alternatives to the standard single-field slow-roll model, which predicts a nearly Gaussian distribution, can produce a significant amount of non-Gaussianity (Bartolo et al. 2004; Chen 2010). The most recent analyses of the observational data show some evidence for possible departures from Gaussianity, even if with a low level of significance (Peebles 1983; Desjacques & Seljak 2010; LoVerde & Smith 2011; D'Amico et al. 2011; Komatsu et al. 2011; as also collected in the summary Table 2 by Maio & Iannuzzi 2011). More precisely, slightly positively skewed models are favored.

From a theoretical point of view, the presence of some amount of primordial non-Gaussianity has two main effects, which are then used as efficient constraining tools: it introduces a scale-dependence in the bias factor (e.g. Grinstein & Wise 1986; McDonald 2008; Desjacques et al. 2009; Fedeli et al. 2011; Noreña et al. 2012; Wagner & Verde 2012), and it modifies the abundance and the formation history of rare events (i.e. very low- and high-sigma fluctuations; e.g. Koyama et al. 1999; Zaldarriaga 2000; Grossi et al. 2007, 2008; Wagner et al. 2010; LoVerde & Smith 2011). High redshifts represent an interesting regime to potentially investigate these effects. Indeed, very early structures and primordial mini-haloes hosting the first bursts of star formation are expected to be somehow affected by the presence of primordial non-Gaussianities (as discussed in Maio 2011).

In more detail, due to the sensitivity of the gas cooling capabilities to the underlying matter density field, numerical hydrodynamical simulations have shown that the initially skewed non-Gaussian features could be reflected by the probability distribution function of the high-z cosmic medium (Viel et al. 2009), by a change in the molecular gas evolution and formation epoch of first stars and galaxies (Maio & Iannuzzi 2011; Maio 2011), and by the consequent metal pollution in the Universe (Maio & Khochfar 2012). Furthermore, simple semi-analytical arguments have suggested non-Gaussianity effects on the birth of primordial black holes (e.g. Bullock & Primack 1997; Green & Liddle 1997; Ivanov 1998; Avelino 2005; Hidalgo 2007; Kohri et al. 2008; Bugaev & Klimai 2012; Byrnes et al. 2012), cosmic reionization (Crociani et al. 2009), and hydrogen 21-cm signal (Cooray 2006; Cooray et al. 2008; Pillepich et al. 2007; Joudaki et al. 2011; Chongchitnan & Silk 2012).

In this respect, a key tool for studies of high-redshift environments might be represented by γ-ray bursts (GRBs), powerful explosions emitting γ rays in the $\sim [1\,\mathrm{keV}, 10\,\mathrm{MeV}]$ energy band, mostly distributed around $\sim 0.1 - 1\,\mathrm{MeV}$, as detected by the latest *Fermi-GBM* instrument operating in the [8 keV, 40 MeV] range (Bissaldi et al. 2011).

These bursts have: isotropic equivalent peak luminosities as high as $\sim 10^{54}\,\mathrm{erg\,s^{-1}}$ (the record holder being GRB 080607, Perley et al. 2011); an isotropic angular distribution (Fishman et al. 1994; Paciesas et al. 1999, 2012); and a bimodal duration distribution (Kouveliotou et al. 1993), with most of them lasting for a period longer than 2 seconds (long GRBs), and some of them, detected mostly at low redshift, for a period shorter than 2 seconds (short GRBs).

In the following we will only consider long GRBs (LGRBs), which are supposedly related to the death of massive stars (see extensive reviews by e.g. Piran 2004; Mészáros 2006) and, therefore, they are indicators of the local star formation episodes (e.g. Jakobsson et al. 2005; Nuza et al. 2007; Lapi et al. 2008; Yüksel et al. 2008; Kistler

et al. 2009; Butler et al. 2010; Campisi et al. 2011; Mannucci et al. 2011; Ishida et al. 2011; Elliott et al. 2012; Robertson & Ellis 2012; Michałowski et al. 2012).

Typical γ-ray bursts have long-lasting afterglows at lower frequencies, from the X-rays to the radio band due to scattering with the surrounding ambient medium (Paczynski 1991; Dermer 1992), and are theoretically explained by the "collapsar model" (Woosley 1993; Wang & Wheeler 1998; Meszaros et al. 1999; Woosley & Heger 2012): a massive black-hole stellar remnant – probably a Wolf-Rayet star (but see Baron 1992; Yoon et al. 2010) – accreting stellar mass from a disk (Popham et al. 1999; Fryer et al. 1999; Narayan et al. 2001; Yoon & Langer 2005; De Colle et al. 2012) at a rate of $\sim 0.01 - 10\,\mathrm{M_\odot/s}$, and accompanied by a collimated-jet emission with a few degree opening angle (e.g. Waxman 1997; Rhoads 1997; Sari et al. 1998; Wang & Wheeler 1998; Schmidt 1999, 2001).

Due to additional factors, like asymmetric explosions or stellar rotation (e.g. Sollerman et al. 2005; Thöne et al. 2008; Östlin et al. 2008), only a small fraction of SNe, $\sim 10^{-2} - 10^{-3}$ (Fruchter et al. 2006; Yoon et al. 2006; Bissaldi et al. 2007; Soderberg et al. 2010; Grieco et al. 2012), can result into a LGRB. However, also taking into account such effects, there is still significant lack of knowledge of some important details, like the minimum mass for GRB black-hole progenitors, that is highly debated and expected to lie between typical SN limits of $\sim 25 - 40\,\mathrm{M_\odot}$ (see also recently proposed upper values of even $\sim 60\,\mathrm{M_\odot}$ in Georgy et al. 2012).

The uniquely bright luminosities of GRBs facilitate their detection up to very high redshift, as shown by the three bursts spectroscopically confirmed at $z > 6$, i.e. GRB 050904 at $z = 6.3$ (Kawai et al. 2006), GRB 080913 at $z = 6.7$ (Greiner et al. 2009), and GRB 090423 at $z = 8.2$ (Salvaterra et al. 2009; Tanvir et al. 2009), and by the case of GRB 090429B, having a photometric redshift of $z \sim 9.4$ (Cucchiara et al. 2011).

High-redshift GRBs are a powerful and, in some cases, a unique tool to study the Universe at the early stages of structure formation and can provide fundamental information about the environment of their own *hosting galaxies* like:

- metallicity and dust content (Savaglio et al. 2005; Savaglio 2006; Nuza et al. 2007; Fynbo et al. 2008; Savaglio et al. 2009; Mannucci et al. 2011; Campisi et al. 2011; Niino et al. 2011);
- neutral-hydrogen fraction (Nagamine et al. 2008; McQuinn et al. 2008; McQuinn & et al. 2009; Gallerani et al. 2008; Mirabel et al. 2011; Robertson & Ellis 2012);
- local inter-galactic radiation field (Inoue et al. 2010);
- early cosmic magnetic fields (Takahashi et al. 2011);
- stellar populations (Bromm & Loeb 2006; Campisi et al. 2011; de Souza et al. 2011; Salvaterra et al. 2012);

In the present work, we argue that GRBs can be additionally used as cosmological probe of the amount of non-Gaussianity present in the primordial density field. In fact, they are sensitive to the underlying cosmological model through the first episodes of the cosmic star formation history.

We will show how GRBs trace the matter distribution at high redshift by performing a detailed analysis of the GRB rate in different non-Gaussian scenarios, with the help of N-body, hydrodynamic, chemistry simulations of early structure formation (Maio & Iannuzzi 2011). In the simulated volumes, star formation is addressed on the basis of the local thermodynamical properties of the collapsing gas, by consistently following its density, temperature and chemical composition, and by taking into account stellar evolution and feedback effects. The resulting star formation rate (SFR) and

the adopted initial mass function (IMF) for the stellar populations tracked during the runs are used to determine the expected GRB formation rate density in the various cases, and hence the integrated GRB rate (R), for both metal-poor population III (hereafter, popIII) regime and metal-enriched population II-I (hereafter, popII-I) regime.

The paper is structured as follows. In Sect. 2 we describe the numerical simulations used in our study; in Sect. 3 we present the adopted model for GRB evolution (Sect. 3.1), its validation (Sect. 3.2), and the consequencies for non-Gaussian models (Sect. 3.3); finally, in Sect. 4 we discuss and summarize our findings and conclude. In the following, when mentioning GRBs we will refer to LGRBs.

2 NUMERICAL SIMULATIONS

In the present paper, we will consider a set of numerical N-body, hydrodynamical, chemistry simulations with two different box sizes starting from initial conditions with a different level of primordial non-Gaussianity. A more detailed description of the simulations can be found in Maio & Iannuzzi (2011). Local non-Gaussianities were included in the initial conditions by adding second-order perturbations to the Bardeen gauge-invariant potential (e.g. Salopek & Bond 1990):

$$\Phi = \Phi_{\mathrm{L}} + f_{\mathrm{NL}} \left[\Phi_{\mathrm{L}}^2 - < \Phi_{\mathrm{L}}^2 > \right], \qquad (1)$$

where Φ_{L} is the *linear* Gaussian part, and f_{NL} the dimensionless coupling constant controlling the magnitude of the deviations from Gaussianity in the large-scale-structure formalism.

The simulations were performed by using a modified version of the parallel tree-PM/SPH Gadget code (Springel 2005), which includes gravity and hydrodynamics, with radiative gas cooling both from molecular and atomic (resonant and fine-structure) transitions (Maio et al. 2007), a multi-phase model for star formation (Springel & Hernquist 2003), UV background radiation (Haardt & Madau 1996), wind feedback (Springel & Hernquist 2003; Aguirre et al. 2001), chemical network for e^-, H, H^+, H^-, He, He^+, He^{++}, H_2, H_2^+, D, D^+, HD, HeH^+ (e.g. Yoshida et al. 2003; Maio et al. 2006, 2007, 2009; Maio 2009; Maio et al. 2010, and references therein), and metal (C, O, Mg, S, Si, Fe) pollution from popIII and/or popII-I stellar generations, ruled by a critical metallicity threshold of $Z_{crit} = 10^{-4} Z_\odot$ (see discussion in Tornatore et al. 2007; Maio et al. 2010, 2011). The cosmological parameters are fixed by assuming a flat concordance ΛCDM model with matter density parameter $\Omega_{0,\mathrm{m}} = 0.3$, cosmological-constant density parameter $\Omega_{0,\Lambda} = 0.7$, and baryon density parameter $\Omega_{0,\mathrm{b}} = 0.04$; the present Hubble parameter is fixed to $H_0 = 100\, h\,\mathrm{km/s/Mpc}$, with $h = 0.7$. Finally, the matter power spectrum has a spectral index $n = 1$ and is normalized assuming that the mass variance within 8 Mpc/h-radius sphere is $\sigma_8 = 0.9$.

A Salpeter IMF with mass range [0.1, 100] $\mathrm{M}_\odot$ was adopted for the popII-I regime, while a top-heavy IMF with short-lived stars in the mass range [100, 500] $\mathrm{M}_\odot$ was assumed for the popIII regime (see literature for further studies on the expected range of massive popIII stars: Abel et al. 2002; Yoshida et al. 2003; Inayoshi & Omukai 2012; or low-mass popIII stars: Yoshida 2006; Yoshida et al. 2007; Campbell & Lattanzio 2008; Suda & Fujimoto 2010; and the impacts of the different assumptions: Maio et al. 2010).

Massive stars die as SN or as pair-instability SN (PISN) in the range [8, 40] $\mathrm{M}_\odot$ and [140, 260] $\mathrm{M}_\odot$, respectively, polluting the surrounding medium and enhancing the transition from a metal-poor to a metal-rich regime (e.g. Tornatore et al. 2007; Maio et al. 2010, 2011). Black-hole remnants form from stellar masses in the ranges [40, 100] $\mathrm{M}_\odot$ (popII-I progenitors), [100, 140] $\mathrm{M}_\odot$ (popIII progenitors), and [260, 500] $\mathrm{M}_\odot$ (popIII progenitors).

To follow with sufficient accuracy all the relevant scales at the different cosmological epochs, we consider two sets of simulations.

The first one assumes small boxes with side of 0.5 Mpc/h, and allows us to resolve the gas behaviour down to $\sim$ pc scales at $z \sim 9 - 30$ (Maio & Khochfar 2012), with gas and dark-matter mass resolutions of 42.35 $\mathrm{M}_\odot/h$ and 275.28 $\mathrm{M}_\odot/h$, respectively, and comoving softening of 4 pc/h.

The box size of the second set is much larger, 100 Mpc/h, so that we can resolve galactic $\sim$ kpc scales at lower redshift (Maio et al. 2011), since gas and dark-matter mass resolutions are 3.39×10^8 $\mathrm{M}_\odot/h$ and 2.20×10^9 $\mathrm{M}_\odot/h$, respectively, and the comoving softening is 7.8 kpc/h.

For both sets of simulations, different levels of primordial non-Gaussianity have been considered, namely $f_{\mathrm{NL}} = 0, 10, 50, 100$, and 1000. We highlight that current data seem to suggest positive f_{NL} values, between 0 and 100 (e.g. Komatsu et al. 2011), but in the present work we will consider the $f_{\mathrm{NL}} = 1000$ case as well, as an extreme example. For further details we refer to Maio & Iannuzzi (2011).

The star formation rate for both stellar population regimes extracted from these simulations will represent the fundamental input for our estimates of the GRB rates, as described in the following sections. For the sake of clarity, in Fig. 1 we re-propose the redshift evolution of the star formation rate densities derived from our ten runs and widely discussed in Maio & Iannuzzi (2011). These curves are the starting point of our following analyses.

3 CALCULATION OF THE GRB RATES

In the following section we will present the results for the GRB rates expected from our simulations. Our starting point is the comoving SFR density, $\dot{\rho}_\star$, tracked by the different runs as a function of z (Maio et al. 2010; Maio & Iannuzzi 2011; Maio 2011), from which we compute the evolution of the GRB formation rate density, $\dot{n}_{\mathrm{GRB}}$, and hence the corresponding integrated GRB rate, R.

We will proceed as follows: in the first place, we will present a phenomenological model describing the redshift evolution of GRBs as observed by *Swift* (Sect. 3.1); then we will validate it against observational data at $z \geqslant 6$ (Sect. 3.2), i.e. the epoch when the effects of primordial non-Gaussianities are expected to play a major role; and eventually we will apply it to an ideal instrument that is assumed to detect all the GRBs produced in the different cosmological scenarios (Sect. 3.3).

3.1 Model description

The basic features of the model are presented in Sect. 3.1.1, followed by the derivation of the best-fitting values for the model free parameters in Sect. 3.1.2. We stress that the parameters of the model are dependent on the whole cosmic star formation history, and, therefore, they do depend on the f_{NL} values, too.

3.1.1 Formalism

The expected redshift distribution of "observed" GRBs can be computed once the GRB luminosity function (LF) and the GRB forma-
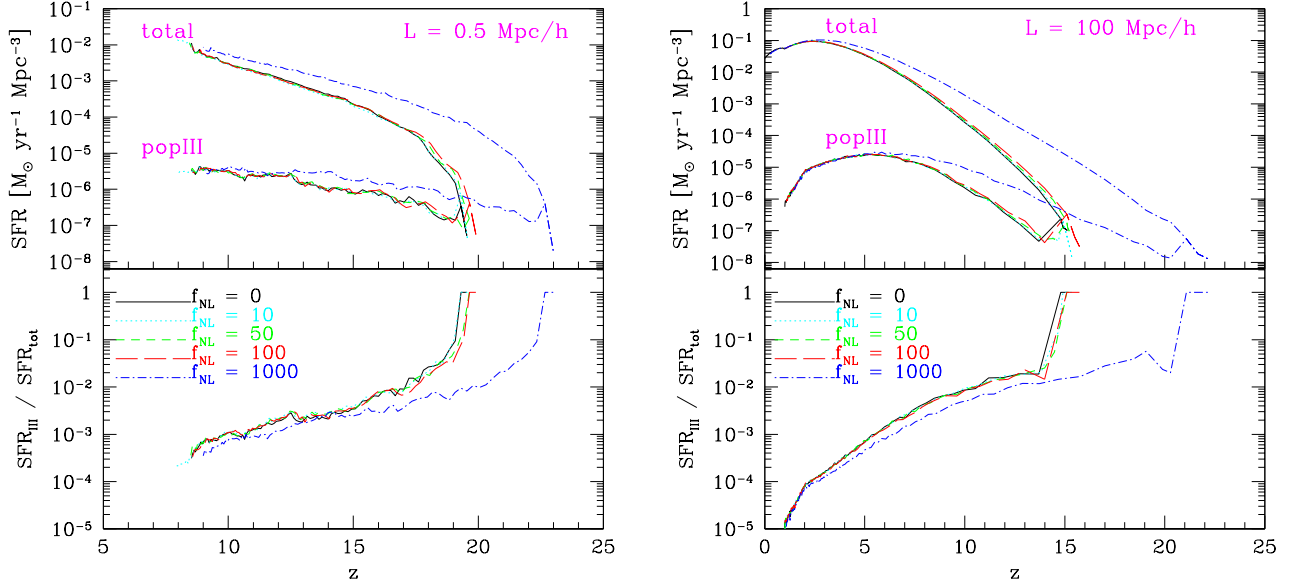
Figure 1. *Top panels*: total and popIII star formation rate density evolution as a function of redshift, z, for the small (left) and the large (right) boxes. Different lines refer to $f_{NL} = 0$ (solid black lines), 10 (dotted cyan lines), 50 (short-dashed green lines), 100 (long-dashed red lines), and 1000 (dot-dashed blue lines). *Bottom panels*: ratio between the popIII and the total star formation rate. The plots are taken from Maio & Iannuzzi (2011).

tion history have been specified (e.g. Porciani & Madau 2001; Firmani et al. 2004; Natarajan et al. 2005; Guetta et al. 2005; Daigne et al. 2006; Salvaterra & Chincarini 2007; Salvaterra et al. 2009; Dai 2009; Wanderman & Piran 2010; Cao et al. 2011; Salvaterra et al. 2012).

We briefly recap here the adopted formalism and refer the interested reader to Salvaterra & Chincarini (2007); Salvaterra et al. (2009, 2012) for more details.

The observed peak photon flux, P, emitted by an isotropically radiating source at redshift z and corresponding luminosity distance $d_L(z)$, as detected in the energy band $E_{\min} < E < E_{\max}$, is

$$P = \frac{(1+z)}{4\pi d_L^2(z)} \int_{(1+z)E_{\min}}^{(1+z)E_{\max}} S(E)\, \mathrm{d}\, E, \tag{2}$$

where $S(E)$ is the differential rest-frame photon luminosity of the source. To describe the typical burst spectrum we adopt a "Band" function with low- and high-energy spectral indices equal to -1 and -2.25, respectively (see also Band et al. 1993; Preece et al. 2000; Kaneko et al. 2006).

The spectrum normalization is obtained by imposing that the isotropic-equivalent peak luminosity is

$$L = \int_{1\,\mathrm{keV}}^{10\,\mathrm{MeV}} E\, S(E)\, \mathrm{d}E. \tag{3}$$

To estimate the peak energy of the spectrum, E_p, for a given L, we correlate E_p and L as done in Yonetoku et al. (2004); Nava et al. (2012); Ghirlanda et al. (2012).

Given a normalized GRB LF, $\psi(L)$, the observed number rate of bursts (in yr^{-1}) at redshift z with peak photon flux, P, between P_1 and P_2 is

$$\dot{N}(z) \equiv \frac{\mathrm{d}N_{P_1 < P < P_2}(z)}{\mathrm{d}t} = \int_z^\infty \mathrm{d}z' \frac{\mathrm{d}V(z')}{\mathrm{d}z'} \frac{\dot{n}_{\mathrm{GRB}}(z')}{(1+z')}$$
$$\times \int_{L_{P_1}(z')}^{L_{P_2}(z')} \psi(L')\mathrm{d}L', \tag{4}$$

where the factor $(1+z')^{-1}$ accounts for cosmological time dilation,

$$\frac{\mathrm{d}V(z)}{\mathrm{d}z} = \mathrm{d}\Omega\, d_c^2(z)\, \frac{c}{H(z)} \tag{5}$$

is the comoving volume element, $\mathrm{d}\Omega$ is the solid angle $d_c(z)$ is the comoving distance, $H(z)$ is the expansion parameter (for more explicit details see e.g. Weinberg 1972; Hogg 1999), c is the speed of light, and $\dot{n}_{\mathrm{GRB}}(z)$ is the actual comoving GRB formation rate density as a function of redshift.

Here, we assume that GRBs are good tracers of star formation, and thus that the GRB formation rate density is directly proportional to the SFR density (see further discussion in Sect. 4), i.e.

$$\dot{n}_{\mathrm{GRB}}(z) \equiv k\dot{\rho}_\star(z), \tag{6}$$

where the normalization constant, k (whose dimensions are the inverse of a mass), incorporates further not-well-known effects, like GRB beaming (Frail et al. 2001; Panaitescu & Kumar 2001; Rossi et al. 2002; Ghirlanda et al. 2007), efficiencies (Fruchter et al. 2006; Yoon et al. 2006; Bissaldi et al. 2007; Soderberg et al. 2010; Grieco et al. 2012), and black-hole production probability (depending on the adopted IMF).

We will adopt (see next section for more details) a normalized GRB LF described by a single power-law with slope ξ and decreasing exponentially below a characteristic luminosity, $L_\star$,

$$\psi(L) \propto \left(\frac{L}{L_\star}\right)^{-\xi} \exp\left(-\frac{L_\star}{L}\right). \tag{7}$$
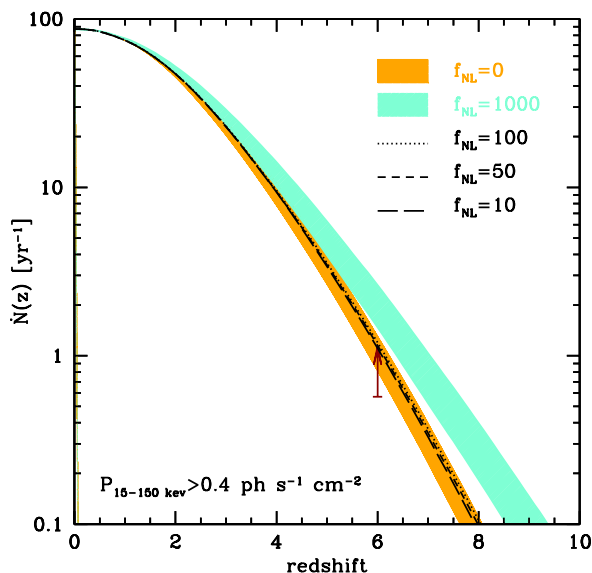
Figure 2. Redshift evolution of the observed number rate of GRBs, $\dot{N}$, at the sensitivity of *Swift* instrument, corresponding to a peak flux of 0.4 ph s^{-1} cm^{-2} in the [15, 150] keV band, and for the *Swift* field of view $\Delta\Omega_s = 1.4$ sr. Model results for f$_{NL} = 0$ and f$_{NL}$=1000 are shown as dark orange and light blue shaded regions, respectively, taking into account the errors on the evolution parameter. The trends (without errors) for the models with $f_{NL} = 10, 50, 100$ are shown with long-dashed, short-dashed, and dotted lines, respectively. The arrow refers to the lower limit on the rate of GRBs at $z > 6$, imposed by the four confirmed detections at these redshifts (see text).

Then, we consider the possibility that the GRB LF evolves by setting $L_\star(z) = L_{\star,0}(1+z)^\delta$, where $L_{\star,0}$ is the characteristic luminosity at $z = 0$, and δ is the evolution parameter.

For simplicity, the normalization of $\psi(L)$ is included in k, and it is fixed when the GRB number rate in equation (4) is normalized to the rate observed at $z = 0$.

From the previous relations we can finally compute the GRB rate (in units of yr^{-1} sr^{-1}), R, as:

$$R(z) = \frac{d\dot{N}(z)}{d\Omega}, \qquad (8)$$

i.e. by taking the derivative with respect to the solid angle of the GRB number rate in equation (4).

3.1.2 Parameter estimation

The values of the free parameters of the model (i.e. $L_{\star,0}$, ξ, k and δ) are optimized separately for all the models, by using the SFRs obtained from the different cases in the 100 Mpc/h-size boxes.

We proceed by minimizing the C-stat function (Cash 1979), jointly fitting the observed differential number counts in the [50, 300] keV band of BATSE (Stern et al. 2001) and the observed redshift distribution of bursts in a redshift complete subsample between $z = 0.13$ and $z = 5.47$ of *Swift* bursts with photon fluxes in excess of 2.6 ph s^{-1} cm^{-2} in the *Swift* [15, 150] keV band (for more details see Salvaterra et al. 2012).

While the redshift complete *Swift* subsample provides a powerful test for the existence and the redshift evolution of the long GRB population, the fit to the BATSE number counts allows to obtain the

normalization k and to better constrain the GRB LF free parameters. It is worth noting that the same best-fit parameters provide a good fit also to the *Swift* differential peak-flux number counts once the energy band ([15, 150] keV), the field of view ($\Delta\Omega_s = 1.4$ sr), and the observing lifetime of *Swift* are considered (Salvaterra & Chincarini 2007).

The best-fit values together with their 1-σ confidence levels are provided for the different values of f_{NL} in Table 1.

We note that since the star formation rate densities are similar for $f_{NL} \leqslant 100$, the best-fit parameters obtained do not differ significantly with respect to the Gaussian case. Also in the most extreme case f_{NL}=1000 the GRB LF best-fit parameters are still consistent with those obtained in the Gaussian cosmology. However, in this case, the normalization k and the evolution parameter δ are affected by the different shape of the cosmic SFR. This was indeed expected: because of the enhanced SFR at high redshift in the f_{NL}=1000 model, a slightly lower evolution is required to reproduce the observed redshift distribution of the complete sample of bright *Swift* GRBs and, consequently, also a different normalization is found.

The LF of popIII GRBs is completely unknown. To compute their rate, we follow Campisi et al. (2011) and assume that popIII GRBs can be described by equation (7) with $\xi = 1.7$ and $L_\star = 10^{54}$ erg s^{-1} constant in redshift (i.e. $L_{\star,0} = 10^{54}$ erg s^{-1} and $\delta = 0$) (Toma et al. 2011). The normalization is then obtained by imposing that none of the ~ 500 GRBs detected by *Swift* so far were powered by popIII star explosions. We checked that our results do not change significantly when varying ξ between 1.5 and 2 and $\log(L_{\star,0}/\text{erg s}^{-1})$ between 53 and 55.

3.2 Validation from the *Swift* redshift distribution

Before calculating the GRB rate expected for different cosmologies, we test the validity of our theoretical model by means of the *Swift* data. We remind that, as of today, the *Swift* instrument has detected 604 GRBs in a lifespan of about 7 years, and the redshift complete (sub-)samples that have been extracted so far have only several tens of data points (see Perley et al. 2009; Greiner et al. 2011; Salvaterra et al. 2012; Hjorth et al. 2012).

Fig. 2 reports the redshift evolution of all models expected at the *Swift* sensitivity, corresponding to a peak photon flux of 0.4 ph s^{-1} cm^{-2} in the [15, 150] keV band. The *Swift* field of view of $\Delta\Omega_s = 1.4$ sr has been assumed. If we compare the f_{NL}=0 and 1000 cases, it is evident that significant differences arise at $z \gtrsim 6$, where $\dot{N}$ changes by at least factor of ~ 2. At lower redshift the two distributions are very similar and possible differences fall within the uncertainties (shaded regions) on the evolution parameter, δ. Indeed, the upper and lower bounds of the shaded regions correspond to the evolution obtained by fitting the complete *Swift* sample with the maximum and minimum values of δ as quoted in Table 1. We note that in principle an instrument like *Swift* can distinguish between a Gaussian and a highly non-Gaussian model simply on the basis of the rate of GRB detections at high z.

The four confirmed detections at $z > 6$ (GRB 050904 at $z = 6.3$ by Kawai et al. 2006; GRB 080913 at $z = 6.7$ by Greiner et al. 2009; GRB 090423 at $z = 8.2$ by Salvaterra et al. 2009,Tanvir et al. 2009; GRB 090429B at $z \simeq 9.4$ by Cucchiara et al. 2011) correspond to a rate of $\dot{N}(6) = 0.57 \pm 0.28$ GRBs per year, derived by using the entire timespan of *Swift* (~ 7 years). At face value, this is fully consistent with the predictions that our model provides for the Gaussian case. Moreover, since the GRB redshift distribution for mildly non-Gaussian models does not differ significantly in

Model	$\log_{10}(\,k\,[\mathrm{M}_\odot{}^{-1}]\,)$	$L_{\star,0,51}$	ξ	δ	C-stat
$f_{\mathrm{NL}}{=}0$	$-7.70^{+0.09}_{-0.06}$	$0.17^{+0.23}_{-0.10}$	$2.04^{+0.15}_{-0.11}$	$2.59^{+0.63}_{-0.57}$	29
$f_{\mathrm{NL}}{=}10$	$-7.70^{+0.09}_{-0.06}$	$0.18^{+0.24}_{-0.10}$	$2.04^{+0.15}_{-0.11}$	$2.57^{+0.62}_{-0.57}$	29
$f_{\mathrm{NL}}{=}50$	$-7.70^{+0.09}_{-0.06}$	$0.18^{+0.24}_{-0.10}$	$2.04^{+0.15}_{-0.11}$	$2.57^{+0.62}_{-0.57}$	29
$f_{\mathrm{NL}}{=}100$	$-7.70^{+0.09}_{-0.06}$	$0.19^{+0.25}_{-0.11}$	$2.04^{+0.15}_{-0.11}$	$2.53^{+0.62}_{-0.56}$	30
$f_{\mathrm{NL}}{=}1000$	$-7.75^{+0.10}_{-0.06}$	$0.36^{+0.48}_{-0.21}$	$2.10^{+0.20}_{-0.13}$	$2.08^{+0.56}_{-0.50}$	30

Table 1. Best-fit values and 1-σ errors for the free parameters of the GRB model, computed for the different cosmologies. From left to right the columns refer to the value of: f_{NL}; the GRB normalization in $[\mathrm{M}_\odot{}^{-1}]$, k; the characteristic luminosity at $z=0$ in $[10^{51}\ \mathrm{erg\ s}^{-1}]$, $L_{\star,0,51}$; the slope parameter of the GRB LF, ξ; the redshift evolution parameter of the characteristic luminosity in the GRB LF, δ; the total C-stat value (i.e., the sum of the C-stat values obtained from the fit of the BATSE and *Swift* dataset) – for more details see Salvaterra et al. (2012). The total number of data points used to perform the fit is 33.

the redshift range probed by *Swift*, the observed high-z rate is also consistent with any non-Gaussian model with a positive but smaller than $\sim 100\ f_{\mathrm{NL}}$.

However, we have to remind that the observed value for $\dot{N}(z)$ at $z=6$ is a lower limit for the rate of high-z GRB detections with *Swift*, since some bursts at $z>6$ could be hidden among the large fraction ($\sim 2/3$) of GRBs for which the redshift has not been measured. For this reason, the previous constraint seems to rule out very negative values of f_{NL} that would fall below the aforementioned limit.

A strong upper limit of $\leqslant 14\%$ on the fraction of $z>6$ GRBs detected by *Swift* has been recently determined by Jakobsson et al. (2012)[1]. Considering the 604 GRBs constituting the current *Swift* sample, this corresponds to at most 85 GRBs at $z>6$, and to a rate of $\dot{N}(6) \lesssim (12\pm1)\ \mathrm{yr}^{-1}$ (as this value is quite large, we do not show it in Fig. 2).

The $f_{\mathrm{NL}}{=}1000$ case and larger values, already excluded by CMB analyses (Komatsu et al. 2011), lie off the observed rate by one order of magnitude or more.

The previous considerations are based on the data point for the GRB rate at $z \simeq 6$, but higher-z data, and larger, redshift complete samples (e.g. Perley et al. 2009; Greiner et al. 2011; Salvaterra et al. 2012; Hjorth et al. 2012) together with a better knowledge of the GRB luminosity function and of its redshift evolution, are needed in order to reduce error bars and to put tighter constraints on the amount of primordial non-Gaussianity on the basis of the observed GRB redshift distribution. More precisely, in order to discriminate, at redshift $z=6$, between e.g. the $f_{\mathrm{NL}}=0$ and the $f_{\mathrm{NL}}=1000$ cases (whose number rates at $z=6$ differ by a factor of ≈ 2), with a 3σ confidence level, one should have a redshift complete sample of roughly 800 GRBs (Poissonian errors have been assumed, and a current *Swift* number rate of $\dot{N}(0)=88\ \mathrm{yr}^{-1}$, according to Fig. 2). Such a large sample would also allow us to constrain the GRB LF quite accurately and then strongly reduce the error bars. A confidence level of 1σ would require a smaller redshift complete sample of about 200 GRBs.

3.3 Resulting GRB rates from the simulated cosmologies

After the validation of the model (Sect. 3.2) performed by exploiting the calibration of the GRB rates against *Swift* data (Sect. 3.1.1

---

[1] We stress that the upper limit at $z=6$ of 14% suggested by Jakobsson et al. (2012) refers to a subsample of 69 *Swift* bursts and is obtained by assuming that the GRBs that could not be identified as low-redshift are actually at $z \geqslant 6$. Thus, the value of 14% must be taken as a very strong upper limit.

and 3.1.2), we now apply it to different non-Gaussian cosmologies to derive count predictions as a function of z. Note that we will assume the normalization derived from the simulations with 100 Mpc/h-side boxes for the small 0.5 Mpc/h-side boxes, as well. In fact, the latter are not run down to $z \sim 0$ and thus can not be used for normalization purposes.

We stress that the following results are obtained by assuming an ideal instrument, that is able to detect all the GRBs at high redshift. This is important to note, because, independently of the overall normalization, the main effects of primordial non-Gaussianities on GRBs are expected to be originated by the differences shown in the redshift evolution of the SFRs (see Maio & Iannuzzi 2011) and, hence, in the different GRB rates in the various models.

3.3.1 Evolution of the GRB rates

In Fig. 3 we plot the GRB rate, R, for the small 0.5 Mpc/h-size boxes (left panels) and the large 100 Mpc/h-size boxes (right panels). In the top panels, we show the redshift evolution for all the f_{NL} scenarios considered, while in the bottom panels we focus on the relative contribution of the popIII GRB rate (R_{III}) to the total rate, that is widely dominated by popII-I stellar generations, at $z \lesssim 20$.

Besides small differences for the onset times of star formation, due to the different resolutions of the 0.5 and 100 Mpc/h-side boxes (see details on resolution issues in Maio et al. 2010; Maio & Iannuzzi 2011), in both small and large volumes the effects due to the presence of primordial non-Gaussianities are visible at $z \gtrsim 10-15$, while the rates eventually converge at later times, when feedback mechanisms start dominating the gas behaviour and the resulting star formation.

In the small boxes, deviations from the Gaussian case are evident at earlier times, because these simulations can sample the very small primordial mini-haloes, which are extremely sensitive to the underlying matter distribution (top-left panel). As a consequence, star formation is resolved already at very high redshift and GRB rates of the order of $\sim 10^{-6}\ \mathrm{yr}^{-1}\ \mathrm{sr}^{-1}$ are expected at redshifts as high as $z \sim 23$ for $f_{\mathrm{NL}}= 1000$, and $z \sim 19-20$ for $f_{\mathrm{NL}}= 0-100$. Similar values are reached in the large 100 Mpc/h-side boxes only at $z \sim 20$ for $f_{\mathrm{NL}}= 1000$, and $z \sim 15$ for $f_{\mathrm{NL}}= 0-100$.

These trends are valid for both popII-I and popIII regimes, even though the latter is usually negligible, predicting popIII GRB rates, R_{III}, that, following the behaviour of the popIII SFRs, drop by two orders of magnitude (bottom-left panel).

The larger boxes miss the very small primordial haloes because of lack of resolution, but can sample much larger scales, showing that the effects of primordial non-Gaussianity can still be present at redshift $z \sim 5-10$ (top-right panel), i.e. for the whole first
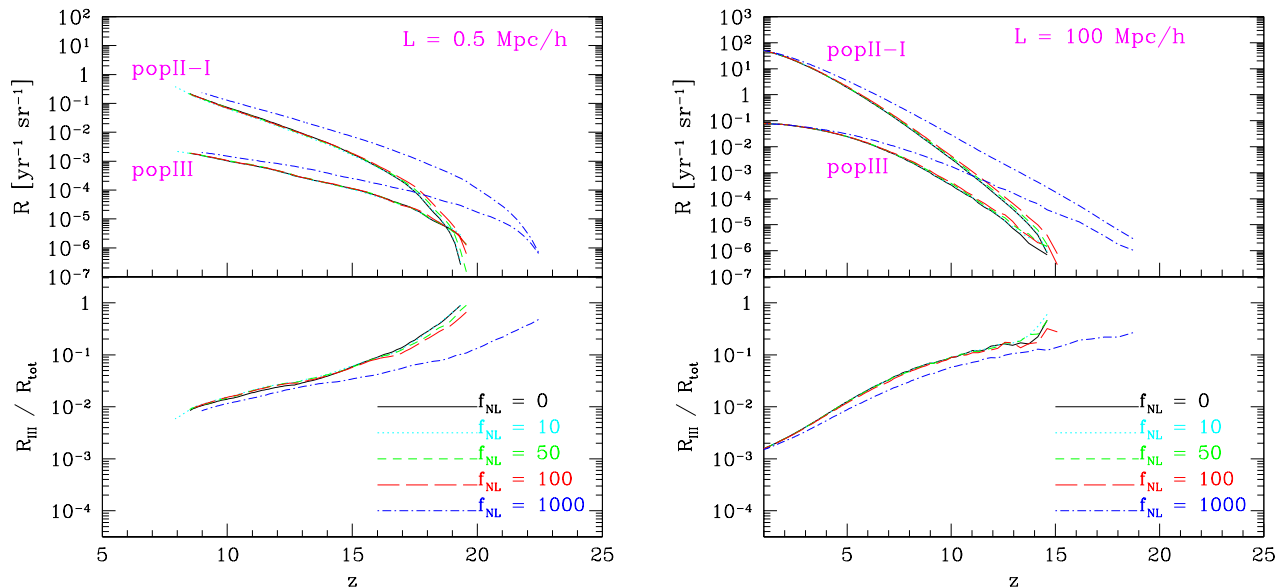
Figure 3. *Top panels*: The expected popII-I and popIII GRB rates, R, in the $0.5\,\mathrm{Mpc}/h$-side boxes (left), and in the $100\,\mathrm{Mpc}/h$-side boxes (right), for models with different primordial non-Gaussianity: f_{NL}= 0 (solid black line), 10 (dotted cyan line), 50 (short-dashed green line), 100 (long-dashed red line), and 1000 (dot-dashed blue line). *Bottom panels*: The corresponding relative contributions of the popIII GRB rates, R_{III}, to the total rate, R, for the different cosmological models.

billion years of the Universe, when the GRB rates should be only one or two orders of magnitude smaller than at present time. Also in these boxes, significant differences in the GRB rates are found only between the $f_{\mathrm{NL}} = 0$ and $f_{\mathrm{NL}} = 1000$ scenarios. This holds for the corresponding popIII contributions (bottom-right panel), as well, and is consistent with what found in the smaller boxes, and with the converging behaviours at redshift below ~ 6.

3.3.2 Comparison of the Gaussian and non-Gaussian models

To directly compare and isolate non-Gaussian effects, in the upper panels of Fig. 4, we plot the ratios between the results for the different non-Gaussian cases and the Gaussian model (f_{NL}=0), for both the 0.5 Mpc/h(left panels) and 100 Mpc/h(right panels) side boxes. Effects of large non-Gaussianities ($f_{\mathrm{NL}} = 1000$) are very well visible at almost any redshift with a rate that is boosted by about ~ 3 orders of magnitude in all boxes, at early epochs. This is due to the fact that in such models, over-densities are heavily biased to larger values, and, therefore, induce an earlier onset of star formation. More precisely, small scales (left panels) seem to depend very tightly on the underlying matter distribution, with enhancements of the GRB rate at $z \sim 20$ by a factor of $\sim 10^3$, 10, 3, and a few per cent, for $f_{\mathrm{NL}} = $ 1000, 100, 50, and 10 respectively. In the latter three cases, feedback mechanisms from on-going star formation are able to reshuffle the gas and drive its hydrodynamical behaviour. As a consequence, the non-Gaussian effects below Mpc scales are almost washed out by redshift $z \sim 15$. The highly non-Gaussian case (f_{NL}=1000), instead, shows more prolonged effects, with variations by a factor ~ 10 at $z \sim 15$, and a factor of ~ 2 at $z \lesssim 10$.

On larger scales (right panels), the ratios are similar for the various non-Gaussian cases, with corresponding delays toward lower redshift in the low-f_{NL} scenarios.

As a conclusion, we can state that the presence of primordial non-Gaussianities in the density fluctuations enhances early GRB rates and has effects up to $z \sim 10$ on Mpc scales, and at least $z \sim 5$ on much larger scales.

To check whether different stellar populations can have different contributions, we can compare the corresponding ratios for popIII GRB rates only. The bottom panels in Fig. 4 readily demonstrate that the popIII GRB rates are less indicative of primordial non-Gaussianities, and less powerful in discriminating different f_{NL} scenarios, mostly for $f_{\mathrm{NL}} \lesssim 100$. The fundamental reason is that the popIII contribution to the SFRs is very noisy due to the short life-times involved (Maio et al. 2010), and thus also the corresponding contribution to the GRB rates present more irregularities compared to the total (popII-I) GRB rates.

Finally, we checked that uncertainties in the unknown popIII IMF[2], in the Z_{crit} value, and in the stellar yields would not lead to significant differences for the previous results (see also related discussions in Maio et al. 2010; Maio & Iannuzzi 2011). Similarly, changes in the popIII GRB efficiency do not alter the relative effects of non-Gaussianities, since they would correspond just to a different overall normalization.

4 DISCUSSION AND CONCLUSIONS

In this work we have discussed the possibility of using GRBs as possible probe of the presence of primordial non-Gaussianities in the density field. This has been done using the outputs of two sets of N-body, hydrodynamic, chemistry simulations presented in Maio & Iannuzzi (2011) (as also briefly described in Sect. 2).

---

[2] Here we adopted alternatively, as an extreme case, a Salpeter-like popIII IMF.
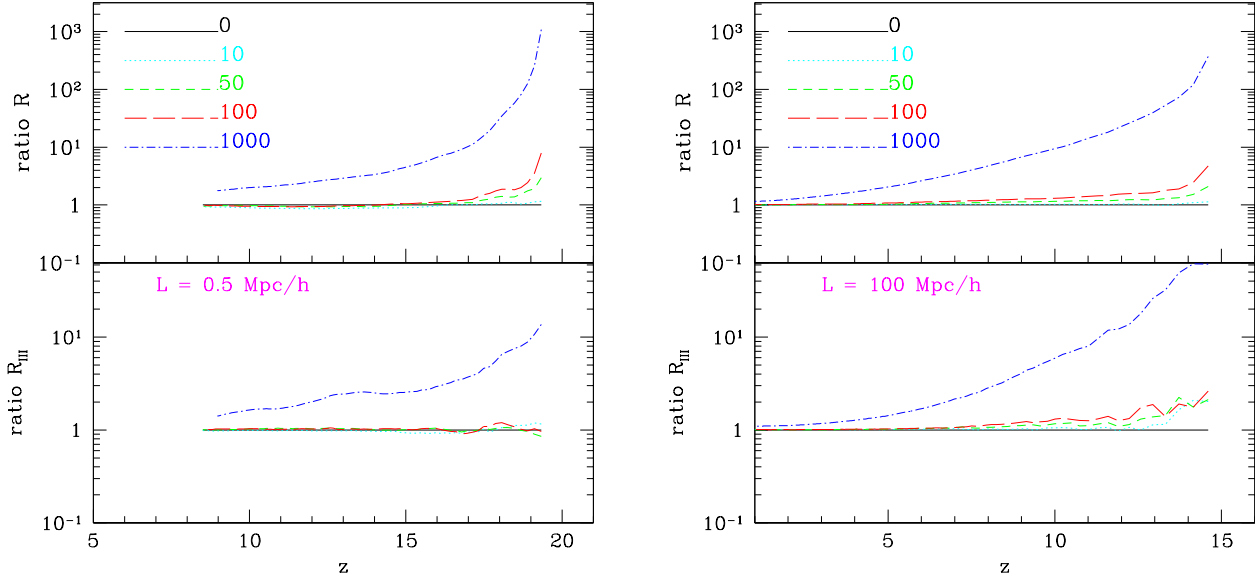
Figure 4. *Top panels*: The ratio between the popII-I GRB rates predicted for the different non-Gaussian models and the Gaussian case. Results for the $0.5 \, \mathrm{Mpc}/h$-side boxes and the $100 \, \mathrm{Mpc}/h$-side boxes are shown in the left and right panels, respectively. Different lines refer to $f_{\mathrm{NL}} = 0$ (solid black line), 10 (dotted cyan line), 50 (short-dashed green line), 100 (long-dashed red line), 1000 (dot-dashed blue line). *Bottom panels*: The corresponding ratios for the popIII GRB rates.

Besides gravity and hydrodynamics, the runs include radiative gas cooling both from molecules and atomic (resonant and fine-structure) transitions, star formation, UV background, wind feed-back, and chemistry evolution for various metal species, for both population III and population II-I stellar generations.

Assuming that long γ-ray bursts are fair tracers of star formation (as suggested by e.g. Nuza et al. 2007; Lapi et al. 2008; Levesque et al. 2010; Campisi et al. 2011; Mannucci et al. 2011; Sanders et al. 2012; Michałowski et al. 2012), we propose to use them as probes of the underlying matter distribution at high redshift, when the possible presence of non-Gaussianity would have the strongest visible effects on the baryon evolution.

By validating our calculations of the GRB rate against *Swift* data, we are able to exclude from the non-linearity parameter space very negative values for f_{NL} (consistently with independent results from CMB data, e.g. Komatsu et al. 2011).

When applying our model to different non-Gaussian scenarios, we find that already at $z \gtrsim 6$ cosmologies with large f_{NL} values present distinctive characteristics compared to those of the Gaussian case, independently from the errors on the LF parameter estimates. Both on large and small scales, at very early times ($z \sim 15 - 20$) the boost in the rate due to non-Gaussianities is $\sim 2 - 3$ orders of magnitudes for $f_{\mathrm{NL}}=1000$, and up to a factor of ~ 10 for $f_{\mathrm{NL}}=100$. Differences of a factor of ~ 2 are still visible for milder values ($f_{\mathrm{NL}} \sim 50$). However, while at small scales we find quick converging trends at lower redshift ($z \sim 9$), determined by the lo-cally on-going star formation and feedback episodes, larger-scale volumes sample bigger objects and thus can retain memory of the primordial matter distribution even at $z \sim 5 - 10$.

These effects are particularly evident on the total GRB rate, that is largely dominated by popII-I stars, while the result for the popIII GRB rate is noisier, mostly for $f_{\mathrm{NL}} \sim 0 - 100$, as a consequence of the corresponding, short-lived, popIII star forming regime (Maio

et al. 2010).

Additional changes in the popIII IMF, yields, Z_{crit}, or the overall normalization of the GRB rates will not alter these findings (see also more discussion in Maio et al. 2010).

We have to recall that, when estimating the level of primordial non-Gaussianity, some difficulties come from the well known de-generacies of f_{NL} with other factors, like cosmological parameters (e.g. the power spectrum normalization σ_8, or the equation-of-state parameter w), or with higher-order effects coming from baryonic matter evolution (e.g. supersonic bulk flows at early times; Tseli-akhovich & Hirata 2010; Maio et al. 2011).

We also warn the reader that the main assumption underlying our formalism is that GRBs are *unbiased* tracers of star formation (Fynbo et al. 2003, 2009; Stanek et al. 2006; Modjaz et al. 2008; Levesque et al. 2010; Levesque et al. 2010). Despite this has been recently supported by several works (see above), arguments for the existence of some possible biases exist in the literature, in particu-lar linked to metallicity selection of the host galaxies (e.g. Langer & Norman 2006). Such effects could alter the intrinsic redshift dis-tribution of GRBs (e.g. Natarajan et al. 2005; Langer & Norman 2006; Salvaterra & Chincarini 2007; Cao et al. 2011; Salvaterra et al. 2012). However, we do not expect this to have significant impacts on the estimated trends of primordial non-Gaussianities. Indeed, any metallicity bias for the GRB formation is not supposed to be too strong, i.e. possible metallicity thresholds for the GRB progenitor stars can not be much lower than $\sim 0.3 \, Z_\odot$ (see Camp-isi et al. 2011).

As shown in this paper, the differences in the GRB rate induced by non-Gaussianities are expected to be significant at very high red-shift. At $z > 6$ most of the galaxies (Salvaterra et al. 2011) and, in particular, most of the GRB progenitors (Salvaterra et al. 2012) have metallicities below this threshold (see also detailed studies in Maio et al. 2010). These studies find that only a small fraction

($\lesssim 5\%$) of galaxies at $z = 6$ has got a metallicity $Z \geqslant 0.3$ Z$_\odot$, rapidly decreasing at higher redshift. Therefore, at least at these early times, our assumption of GRBs as fair tracers of the cosmic SFR is quite solid. Furthermore, we checked that the difference among Gaussian and non-Gausssian models remains unchanged when galaxies with metallicities larger than 0.3 Z$_\odot$ were excluded from our analyses.

We note that estimates of non-Gaussianities (e.g. Komatsu et al. 2011) based on cosmic microwave background and large-scale-structure data seem to support positive f_{NL} values up to ~ 100. This implies that at early epochs we expect an enhancement of the GRB rate up to a factor of 10 with respect to the standard Gaussian case.

We stress that the existence of GRBs at such high redshift is not unlikely, as they are tightly linked to star formation episodes. In principle, they could be observable thanks to their large intrinsic luminosity and longer time dilution of the afterglow. None the less, from an observational point of view, detections of GRB afterglows at very high redshift are complicated by Lyman-α absorption from inter-galactic gas. In fact, for bursts at $z \geqslant 15$, as the ones we are interested in here, no flux can be detected in photometric bands bluer than the K band (at ~ 2.2 μm). At $z > 18$, where the largest differences between Gaussian and mildly non-Gaussian models are expected, observations in the infra-red band are needed. Since follow-up observations of GRB afterglow are generally carried out in optical-NIR bands, extreme high-z GRBs can be missed. However, a small population of extremely dark GRBs (e.g. Greiner et al. 2011), i.e. bursts for which the afterglow remains undetected in spite of early and deep K band observations, has been recently identified (D'Elia & Stratta 2011). While the nature of these GRBs is still matter of debate and alternative explanations for their darkness do exist[3], it is possible that these bursts (or at least one of them) are at $z \geqslant 18$. If confirmed, this could provide evidence in favor of a mildly positive non-Gaussian parameter (f_{NL} in the range $10 - 100$, see Fig. 3). Future detections of extremely dark GRBs (as the ones by D'Elia & Stratta 2011) at redshift $z \gtrsim 20$ and with a substantial rate, of at least $\sim 10^{-6}$ yr^{-1} sr^{-1}, might be an indication of even bigger values for f_{NL}. Naively speaking, a determination of the rate for such GRB would lead to about $\sim (0.1 \pm 0.1)$ yr^{-1}sr^{-1}, but one should also consider that the probability of observing such event is almost as small as $\sim 10^{-3}$, since this is a unique case out of the 604 *Swift* GRBs. In principle, this would imply positive f_{NL} values, but with huge error bars.

However, in order to draw more definitive conclusions and give more stringent constraints much larger high-z GRB complete samples, currently not available in the literature, are required.

ACKNOWLEDGMENTS

[3] Different possible explanations have been proposed, ranging from extreme dust absorptions at $z = 0$ to less extreme, but still demanding, extinctions at $z \simeq 4-5$. Other suggestions invoke a complete revision of the dust extinction curves or even more exotic non-standard models for the GRB afterglow emission (for a more detailed discussion see D'Elia & Stratta 2011).

REFERENCES

Abel T., Bryan G. L., Norman M. L., 2002, Science, 295, 93
Aguirre A., Hernquist L., Schaye J., Katz N., Weinberg D. H., Gardner J., 2001, ApJ, 561, 521
Avelino P. P., 2005, Phys. Rev. D, 72, 124004
Band D., Matteson J., Ford L., Schaefer B., Palmer D., Teegarden B., Cline T., Briggs M., Paciesas W., Pendleton G., Fishman G., Kouveliotou C., Meegan C., Wilson R., Lestrade P., 1993, ApJ, 413, 281
Barkana R., Loeb A., 2001, Phys. Rep., 349, 125
Baron E., 1992, MNRAS, 255, 267
Bartolo N., Komatsu E., Matarrese S., Riotto A., 2004, Phys. Rep., 402, 103
Bissaldi E., Calura F., Matteucci F., Longo F., Barbiellini G., 2007, A&A, 471, 585
Bissaldi E., von Kienlin A., Kouveliotou C., Briggs M. S., Connaughton V., Greiner J., Gruber D., Lichti G., 21 co-authors 2011, ApJ, 733, 97
Bromm V., Loeb A., 2006, ApJ, 642, 382
Bromm V., Yoshida N., 2011, ARA&A, 49, 373
Bugaev E., Klimai P., 2012, Phys. Rev. D, 85, 103504
Bullock J. S., Primack J. R., 1997, Phys. Rev. D, 55, 7423
Butler N. R., Bloom J. S., Poznanski D., 2010, ApJ, 711, 495
Byrnes C. T., Copeland E. J., Green A. M., 2012, ArXiv e-prints, arXiv:1206.4188
Campbell S. W., Lattanzio J. C., 2008, A&A, 490, 769
Campisi M. A., Maio U., Salvaterra R., Ciardi B., 2011, MNRAS, 416, 2760
Campisi M. A., Tapparello C., Salvaterra R., Mannucci F., Colpi M., 2011, MNRAS, 417, 1013
Cao X.-F., Yu Y.-W., Cheng K. S., Zheng X.-P., 2011, MNRAS, 416, 2174
Cash W., 1979, ApJ, 228, 939
Chen X., 2010, Advances in Astronomy, 2010
Chongchitnan S., Silk J., 2012, MNRAS, p. L507
Ciardi B., Ferrara A., 2005, Space Science Reviews, 116, 625
Coles, P. & Lucchin, F. ed. 2002, Cosmology: The Origin and Evolution of Cosmic Structure, Second Edition. Wiley
Cooray A., 2006, Physical Review Letters, 97, 261301
Cooray A., Li C., Melchiorri A., 2008, Phys. Rev. D, 77, 103506
Crociani D., Moscardini L., Viel M., Matarrese S., 2009, MNRAS, 394, 133
Cucchiara A., Levan A. J., Fox D. B., Tanvir N. R., Ukwatta T. N., 32 co-authors 2011, ApJ, 736, 7

Dai X., 2009, ApJ, 697, L68

Daigne F., Rossi E. M., Mochkovitch R., 2006, MNRAS, 372, 1034

D'Amico G., Musso M., Noreña J., Paranjape A., 2011, Phys. Rev. D, 83, 023521

De Colle F., Granot J., López-Cámara D., Ramirez-Ruiz E., 2012, ApJ, 746, 122

de Souza R. S., Yoshida N., Ioka K., 2011, A&A, 533, A32

D'Elia V., Stratta G., 2011, A&A, 532, A48

Dermer C. D., 1992, Physical Review Letters, 68, 1799

Desjacques V., Seljak U., 2010, Classical and Quantum Gravity, 27, 124011

Desjacques V., Seljak U., Iliev I. T., 2009, MNRAS, 396, 85

Elliott J., Greiner J., Khochfar S., Schady P., Johnson J. L., Rau A., 2012, A&A, 539, A113

Fedeli C., Carbone C., Moscardini L., Cimatti A., 2011, MNRAS, 414, 1545

Firmani C., Avila-Reese V., Ghisellini G., Tutukov A. V., 2004, ApJ, 611, 1033

Fishman G. J., Meegan C. A., Wilson R. B., Brock M. N., Horack J. M., Kouveliotou C., Howard S., Paciesas W. S., Briggs M. S., Pendleton G. N., Koshut T. M., Mallozzi R. S., Stollberg M., Lestrade J. P., 1994, ApJS, 92, 229

Frail D. A., Kulkarni S. R., Sari R., Djorgovski S. G., Bloom J. S., Galama T. J., Reichart D. E., Berger E., Harrison F. A., Price P. A., Yost S. A., Diercks A., Goodrich R. W., Chaffee F., 2001, ApJ, 562, L55

Fruchter A. S., Levan A. J., Strolger L., Vreeswijk P. M., 29 co-authors 2006, Nature, 441, 463

Fryer C. L., Woosley S. E., Hartmann D. H., 1999, ApJ, 526, 152

Fynbo J. P. U., Jakobsson P., Möller P., Hjorth J., Thomsen B., Andersen M. I., Fruchter A. S., Gorosabel J., Holland S. T., Ledoux C., Pedersen H., Rhoads J., Weidinger M., Wijers R. A. M. J., 2003, A&A, 406, L63

Fynbo J. P. U., Jakobsson P., Prochaska J. X., 39 co-authors 2009, ApJS, 185, 526

Fynbo J. P. U., Prochaska J. X., Sommer-Larsen J., Dessauges-Zavadsky M., Møller P., 2008, ApJ, 683, 321

Gallerani S., Salvaterra R., Ferrara A., Choudhury T. R., 2008, MNRAS, 388, L84

Georgy C., Ekström S., Meynet G., Massey P., Levesque E. M., Hirschi R., Eggenberger P., Maeder A., 2012, A&A, 542, A29

Ghirlanda G., Ghisellini G., Nava L., Salvaterra R., Tagliaferri G., Campana S., Covino S., D'Avanzo P., Fugazza D., Melandri A., Vergani S. D., 2012, MNRAS, 422, 2553

Ghirlanda G., Nava L., Ghisellini G., Firmani C., 2007, A&A, 466, 127

Green A. M., Liddle A. R., 1997, Phys. Rev. D, 56, 6166

Greiner J., Krühler T., Fynbo J. P. U., Rossi A., Schwarz R., Klose S., Savaglio S., Tanvir N. R., McBreen S., et al. 2009, ApJ, 693, 1610

Greiner J., Krühler T., Klose S., Afonso P., Clemens C., Filgas R., Hartmann D. H., Küpcü Yoldaş A., Nardini M., Olivares E. F., Rau A., Rossi A., Schady P., Updike A., 2011, A&A, 526, A30

Grieco V., Matteucci F., Meynet G., Longo F., Della Valle M., Salvaterra R., 2012, MNRAS, 423, 3049

Grinstein B., Wise M. B., 1986, ApJ, 310, 19

Grossi M., Branchini E., Dolag K., Matarrese S., Moscardini L., 2008, MNRAS, 390, 438

Grossi M., Dolag K., Branchini E., Matarrese S., Moscardini L., 2007, MNRAS, 382, 1261

Guetta D., Piran T., Waxman E., 2005, ApJ, 619, 412

Gunn J. E., Gott III J. R., 1972, ApJ, 176, 1

Guth A. H., 1981, Phys. Rev. D, 23, 347

Haardt F., Madau P., 1996, ApJ, 461, 20

Hidalgo J. C., 2007, ArXiv e-prints, arXiv:0708.3875

Hjorth J., Malesani D., Jakobsson P., Jaunsen A. O., Fynbo J. P. U., Gorosabel J., Krühler T., Levan A. J., Michałowski M. J., Milvang-Jensen B., Møller P., Schulze S., Tanvir N. R., Watson D., 2012, ArXiv e-prints, arXiv:1205.3162

Hogg D. W., 1999, ArXiv Astrophysics e-prints

Inayoshi K., Omukai K., 2012, MNRAS, 422, 2539

Inoue S., Salvaterra R., Choudhury T. R., Ferrara A., Ciardi B., Schneider R., 2010, MNRAS, 404, 1938

Ishida E. E. O., de Souza R. S., Ferrara A., 2011, MNRAS, 418, 500

Ivanov P., 1998, Phys. Rev. D, 57, 7145

Jakobsson P., Björnsson G., Fynbo J. P. U., Jóhannesson G., Hjorth J., Thomsen B., Møller P., Watson D., Jensen B. L., Östlin G., Gorosabel J., Gudmundsson E. H., 2005, MNRAS, 362, 245

Jakobsson P., Hjorth J., Malesani D., Chapman R., Fynbo J. P. U., Tanvir N. R., Milvang-Jensen B., Vreeswijk P. M., Letawe G., Starling R. L. C., 2012, ApJ, 752, 62

Joudaki S., Doré O., Ferramacho L., Kaplinghat M., Santos M. G., 2011, Physical Review Letters, 107, 131304

Kaneko Y., Preece R. D., Briggs M. S., Paciesas W. S., Meegan C. A., Band D. L., 2006, ApJS, 166, 298

Kawai N., Kosugi G., Aoki K., Yamada T., Totani T., Ohta K., Iye M., Hattori T., et al. 2006, Nature, 440, 184

Kistler M. D., Yüksel H., Beacom J. F., Hopkins A. M., Wyithe J. S. B., 2009, ApJ, 705, L104

Kohri K., Lyth D. H., Melchiorri A., 2008, J. of Cosmology and Astroparticle Physics, 4, 38

Komatsu E., Smith K. M., Dunkley J., 18 coauthors 2011, ApJS, 192, 18

Kouveliotou C., Meegan C. A., Fishman G. J., Bhat N. P., Briggs M. S., Koshut T. M., Paciesas W. S., Pendleton G. N., 1993, ApJ, 413, L101

Koyama K., Soda J., Taruya A., 1999, MNRAS, 310, 1111

Langer N., Norman C. A., 2006, ApJ, 638, L63

Lapi A., Kawakatu N., Bosnjak Z., Celotti A., Bressan A., Granato G. L., Danese L., 2008, MNRAS, 386, 608

Levesque E. M., Berger E., Kewley L. J., Bagley M. M., 2010, AJ, 139, 694

Levesque E. M., Kewley L. J., Berger E., Zahid H. J., 2010, AJ, 140, 1557

Levesque E. M., Soderberg A. M., Kewley L. J., Berger E., 2010, ApJ, 725, 1337

Linde A., 1990, Physics Letters B, 238, 160

LoVerde M., Smith K. M., 2011, ArXiv e-prints, arXiv:1102.1439

Maio U., 2009, PhD thesis, Ludwig Maximilian University

Maio U., 2011, Classical and Quantum Gravity, 28, 225015

Maio U., Ciardi B., Dolag K., Tornatore L., Khochfar S., 2010, MNRAS, 407, 1003

Maio U., Ciardi B., Yoshida N., Dolag K., Tornatore L., 2009, A&A, 503, 25

Maio U., Dolag K., Ciardi B., Tornatore L., 2007, MNRAS, 379, 963

Maio U., Dolag K., Meneghetti M., Moscardini L., Yoshida N., Baccigalupi C., Bartelmann M., Perrotta F., 2006, MNRAS, 373, 869

Maio U., Iannuzzi F., 2011, MNRAS, 415, 3021

Maio U., Khochfar S., 2012, MNRAS, 421, 1113

Maio U., Khochfar S., Johnson J. L., Ciardi B., 2011, MNRAS, 414, 1145

Maio U., Koopmans L. V. E., Ciardi B., 2011, MNRAS, pp L197+

Mannucci F., Salvaterra R., Campisi M. A., 2011, MNRAS, 414, 1263

McDonald P., 2008, Phys. Rev. D, 78, 123519

McQuinn M., et al. 2009, in astro2010: The Astronomy and Astrophysics Decadal Survey Vol. 2010 of Astronomy, In Situ Probes of the First Galaxies and Reionization: Gamma-ray Bursts. p. 199

McQuinn M., Lidz A., Zaldarriaga M., Hernquist L., Dutta S., 2008, MNRAS, 388, 1101

Mészáros P., 2006, Reports on Progress in Physics, 69, 2259

Meszaros P., Rees M. J., Wijers R. A. M. J., 1999, New Astronomy, 4, 303

Michałowski M. J., Kamble A., Hjorth J., Malesani D., Reinfrank R. F., 17 co-authors 2012, ArXiv e-prints, arXiv:1205.4239

Mirabel I. F., Dijkstra M., Laurent P., Loeb A., Pritchard J. R., 2011, A&A, 528, A149

Modjaz M., Kewley L., Kirshner R. P., Stanek K. Z., Challis P., Garnavich P. M., Greene J. E., Kelly P. L., Prieto J. L., 2008, AJ, 135, 1136

Nagamine K., Zhang B., Hernquist L., 2008, ApJ, 686, L57

Narayan R., Piran T., Kumar P., 2001, ApJ, 557, 949

Natarajan P., Albanna B., Hjorth J., Ramirez-Ruiz E., Tanvir N., Wijers R., 2005, MNRAS, 364, L8

Nava L., Salvaterra R., Ghirlanda G., Ghisellini G., Campana S., Covino S., Cusumano G., D'Avanzo P., D'Elia V., Fugazza D., Melandri A., Sbarufatti B., Vergani S. D., Tagliaferri G., 2012, MNRAS, 421, 1256

Niino Y., Choi J.-H., Kobayashi M. A. R., Nagamine K., Totani T., Zhang B., 2011, ApJ, 726, 88

Noreña J., Verde L., Barenboim G., Bosch C., 2012, ArXiv e-prints, arXiv:1204.6324

Nuza S. E., Tissera P. B., Pellizza L. J., Lambas D. G., Scannapieco C., de Rossi M. E., 2007, MNRAS, 375, 665

Östlin G., Zackrisson E., Sollerman J., Mattila S., Hayes M., 2008, MNRAS, 387, 1227

Paciesas W. S., Meegan C. A., Pendleton G. N., 15 co-authors 1999, ApJS, 122, 465

Paciesas W. S., Meegan C. A., von Kienlin A., 26 co-authors 2012, ApJS, 199, 18

Paczynski B., 1991, Acta Astronomica, 41, 257

Panaitescu A., Kumar P., 2001, ApJ, 560, L49

Peacock, J. A. ed. 1999, Cosmological Physics. Cambridge University Press

Peebles P. J., Ratra B., 2003, Reviews of Modern Physics, 75, 559

Peebles P. J. E., 1983, ApJ, 274, 1

Peebles, P. J. E. ed. 1993, Principles of Physical Cosmology.

Perley D. A., Cenko S. B., Bloom J. S., Chen H.-W., Butler N. R., Kocevski D., Prochaska J. X., Brodwin M., Glazebrook K., Kasliwal M. M., Kulkarni S. R., Lopez S., Ofek E. O., Pettini M., Soderberg A. M., Starr D., 2009, AJ, 138, 1690

Perley D. A., Morgan A. N., Updike A., Yuan F., Akerlof C. W., Miller A. A., Bloom J. S., Cenko S. B., et al. 2011, AJ, 141, 36

Pillepich A., Porciani C., Matarrese S., 2007, ApJ, 662, 1

Piran T., 2004, Reviews of Modern Physics, 76, 1143

Popham R., Woosley S. E., Fryer C., 1999, ApJ, 518, 356

Porciani C., Madau P., 2001, ApJ, 548, 522

Preece R. D., Briggs M. S., Mallozzi R. S., Pendleton G. N., Paciesas W. S., Band D. L., 2000, ApJS, 126, 19

Press W. H., Schechter P., 1974, ApJ, 187, 425

Rhoads J. E., 1997, ApJ, 487, L1

Robertson B. E., Ellis R. S., 2012, ApJ, 744, 95

Rossi E., Lazzati D., Rees M. J., 2002, MNRAS, 332, 945

Salopek D. S., Bond J. R., 1990, Phys. Rev. D, 42, 3936

Salvaterra R., Campana S., Vergani S. D., Covino S., D'Avanzo P., Fugazza D., Ghirlanda G., Ghisellini G., Melandri A., Nava L., Sbarufatti B., Flores H., Piranomonte S., Tagliaferri G., 2012, ApJ, 749, 68

Salvaterra R., Chincarini G., 2007, ApJ, 656, L49

Salvaterra R., Della Valle M., Campana S., Chincarini G., Covino S., D'Avanzo P., Fernandez-Soto A., Guidorzi C., et al 2009, Nature, 461, 1258

Salvaterra R., Ferrara A., Dayal P., 2011, MNRAS, 414, 847

Salvaterra R., Guidorzi C., Campana S., Chincarini G., Tagliaferri G., 2009, MNRAS, 396, 299

Salvaterra R., Maio U., Ciardi B., Campisi M., 2012, MNRAS, 0

Sanders N. E., Soderberg A. M., Levesque E. M., Foley R. J., Chornock R., Milisavljevic D., Margutti R., Berger E., Drout M. R., Czekala I., Dittmann J. A., 2012, ArXiv e-prints, arXiv:1206.2643

Sari R., Piran T., Narayan R., 1998, ApJ, 497, L17

Savaglio S., 2006, New Journal of Physics, 8, 195

Savaglio S., Glazebrook K., Le Borgne D., 2009, ApJ, 691, 182

Savaglio S., Glazebrook K., Le Borgne D., Juneau S., Abraham R. G., Chen H.-W., Crampton D., McCarthy P. J., Carlberg R. G., Marzke R. O., Roth K., Jørgensen I., Murowinski R., 2005, ApJ, 635, 260

Schmidt M., 1999, ApJ, 523, L117

Schmidt M., 2001, ApJ, 552, 36

Sheth R. K., Tormen G., 1999, MNRAS, 308, 119

Soderberg A. M., Chakraborti S., Pignata G., Chevalier R. A., Chandra P., Ray A., Wieringa M. H., 17 co-authors 2010, Nature, 463, 513

Sollerman J., Östlin G., Fynbo J. P. U., Hjorth J., Fruchter A., Pedersen K., 2005, New Astronomy, 11, 103

Springel V., 2005, MNRAS, 364, 1105

Springel V., Hernquist L., 2003, MNRAS, 339, 289

Stanek K. Z., Gnedin O. Y., Beacom J. F., Gould A. P., Johnson J. A., Kollmeier J. A., Modjaz M., Pinsonneault M. H., Pogge R., Weinberg D. H., 2006, Acta Astronomica, 56, 333

Starobinsky A. A., 1980, Physics Letters B, 91, 99

Stern B. E., Tikhomirova Y., Kompaneets D., Svensson R., Poutanen J., 2001, ApJ, 563, 80

Suda T., Fujimoto M. Y., 2010, MNRAS, pp 444–+

Takahashi K., Inoue S., Ichiki K., Nakamura T., 2011, MNRAS, 410, 2741

Tanvir et al. 2009, Nature, 461, 1254

Thöne C. C., Fynbo J. P. U., Östlin G., Milvang-Jensen B., Wiersema K., Malesani D., Della Monica Ferreira D., Gorosabel J., Kann D. A., Watson D., Michałowski M. J., Fruchter A. S., Levan A. J., Hjorth J., Sollerman J., 2008, ApJ, 676, 1151

Toma K., Sakamoto T., Mészáros P., 2011, ApJ, 731, 127

Tornatore L., Ferrara A., Schneider R., 2007, MNRAS, 382, 945

Tseliakhovich D., Hirata C., 2010, Phys. Rev. D, 82, 083520

Viel M., Branchini E., Dolag K., Grossi M., Matarrese S., Moscardini L., 2009, MNRAS, 393, 774

Wagner C., Verde L., 2012, J. of Cosmology and Astroparticle Physics, 3, 2

Wagner C., Verde L., Boubekeur L., 2010, J. of Cosmology and Astroparticle Physics, 10, 22

Wanderman D., Piran T., 2010, MNRAS, 406, 1944

Wang L., Wheeler J. C., 1998, ApJ, 504, L87

Waxman E., 1997, ApJ, 485, L5

Weinberg S., 1972, Gravitation and Cosmology: Principles and Applications of the General Theory of Relativity

White S. D. M., Rees M. J., 1978, MNRAS, 183, 341

Woosley S. E., 1993, ApJ, 405, 273

Woosley S. E., Heger A., 2012, ApJ, 752, 32

Yonetoku D., Murakami T., Nakamura T., Yamazaki R., Inoue A. K., Ioka K., 2004, ApJ, 609, 935

Yoon S.-C., Langer N., 2005, A&A, 443, 643

Yoon S.-C., Langer N., Norman C., 2006, A&A, 460, 199

Yoon S.-C., Woosley S. E., Langer N., 2010, ApJ, 725, 940

Yoshida N., 2006, New Astronomy Review, 50, 19

Yoshida N., Abel T., Hernquist L., Sugiyama N., 2003, ApJ, 592, 645

Yoshida N., Omukai K., Hernquist L., 2007, ApJ, 667, L117

Yüksel H., Kistler M. D., Beacom J. F., Hopkins A. M., 2008, ApJ, 683, L5

Zaldarriaga M., 2000, Phys. Rev. D, 62, 063510